arXiv:astro-ph/0210166v2 3 Mar 2003

Calculation of optimized apodizers for a Terrestrial Planet Finder coronagraphic telescope

R. Gonsalves

Department of Electrical Engineering and Computer Science

Tufts University, Medford, MA 02155

bobg@eecs.tufts.edu

P. Nisenson

Harvard-Smithsonian Center for Astrophysics

60 Garden St., Cambridge, MA 01803

pnisenson@cfa.harvard.edu

Received _____; accepted _____

ABSTRACT

One of two approaches to implementing NASA's Terrestrial Planet Finder is to build a space telescope that utilizes the techniques of coronagraphy and apodization to suppress diffraction and image exo-planets. We present a method for calculation of a telescope's apodizer which suppresses the side lobes of the image of a star so as to optimally detect an Earth-like planet. Given the shape of a telescope's aperture and given a search region for a detector, we solve an integral equation to determine an amplitude modulation (an apodizer) which suppresses the star's energy in the focal plane search region. The method is quite general and yields as special cases the product apodizer reported by Nisenson and Papaliolios (2001) and the Prolate spheroidal apodizer of Kasdin et al (2002), and Aime et al (2002). We show computer simulations of the apodizers and the corresponding point spread functions for various aperture-detector configurations.

Subject headings: stars: planetary systems — stars: imaging — telescopes

1. Introduction

A central problem in the search for Earth-like planets is to suppress the light from a star so as to reveal a planet which might be 10 to 12 orders of magnitude fainter than the star and might be in quite close to the star. In earlier papers (Nisenson and Papliolios, 2001; Nisenson et al, 2003) we showed that apodizing a telescope pupil reduced the diffraction of a telescope that would allow exo-planet detection. In addition to diffraction suppression, extremely low scattering optical surfaces at frequencies of 3 to 30 cycles/mirror are necessary. Obtaining such low scattering will require a combination of super-polishing and adaptive optic correction. In this paper, we describe a technique for designing an

apodizer that minimizes diffraction in a chosen region of the focal plane while maximizing the throughput of the apodizer.

The image of a star (unaberrated by the atmosphere) is the point spread function (PSF) of the telescope. We want to design a real, non-negative, continuous tone mask, i.e., an apodizer, to place in the aperture (or a relay plane of the aperture) such that the PSF has a compact, central peak with minimal spread beyond the core of the PSF.

This problem was first studied by Slepian & Pollack (1961) in the context of radar, communications, and superresolution. The authors show that the band-limited signal, $\phi(t)$, which has the most energy in time T satisfies the integral equation:

$$\lambda\phi(t) = \int \phi(s)w(s)a(t-s)ds \tag{1}$$

where $w(t)$ is a zero-one function which time-limits $\phi(t)$ to T seconds and the Fourier transform, $A(f)$, of $a(t)$ is another zero-one function which band-limits $\phi(t)$. The solutions (eigenfunctions) of this integral equation are prolate spheroidal (PS) functions and $\phi(t)$ is the eigenfunction with the largest eigenvalue. The authors show that $\phi(t)$, inside T, is identical to its Fourier Transform, $\Phi(f)$, suitably scaled in f. Kaiser (1966) presented an approximation to $\phi(t)$ and subsequent authors (Oppenheim and Schafer, 1989; Aime et al, 2002) have used the Kaiser window because $\phi(t)$ is difficult to compute.

Papoulis (1968) studied the same problem in the optical context and showed that $\Phi(u)$, the Fourier transform of $\phi(t)$, is the optimal one-dimensional apodizer. He showed that the optimal apodizer for a square aperture is the product $\Phi(u)\Phi(v)$, which is the form proposed by Nisenson and Papaliolios (2001). He also shows that the optimal apodizer for a circularly symmetric aperture is a sum of the first and second order Bessel functions. Other authors (Kasdin et al, 2002 and Aime et al, 2001), have shown the optimality of a PS

apodizer. Kasdin et al (2002) suggest a PS-shaped, binary aperture with the key advantage that the binary aperture may be easier to manufacture.

In this paper we present an iterative calculation of an optimal apodizer. The method does not require the Kaiser approximation and it can accommodate any special features of the measurement process, such as the likely position of a planet in reference to its star. We use a very simple iterative procedure to calculate the apodizer, an iterative algorithm that has its roots in linear system theory and is closely related to the well-known Gerchberg-Saxton algorithm (Gerchberg and Saxton, 1972).

2. The Algorithm

We use the method of alternating projections which was introduced by von Neumann (1950). We write Equation (1) in the compact form

$$\lambda\phi = R\phi, \tag{2}$$

where R is an operator, sometimes called the kernel. R space-limits the two-dimensional function $\phi(x, y)$ with a specified spatial mask, $w(x, y)$, then band-limits it with a specified spatial frequency mask, $A(u, v)$. The latter is determined by the shape of the aperture.

To solve Eq. (2) we repeatedly impose R on an initial $\phi(x, y)$ until Eq. (2) is satisfied. More specifically, we calculate

$$f(x, y) = \phi(x, y)w(x, y), \tag{3}$$

then we calculate the Fourier transform of f(x,y), namely F(u,v), and calculate

$$\Phi(u,v) = F(u,v)A(u,v). \tag{4}$$

The inverse Fourier transform of $\Phi(u,v)$ is $\phi(x,y)$, which completes one iteration of the algorithm.

We rely on the fact that n iterations will produce an expansion of $\phi(x,y)$ in eigenfunctions of Eq. 2 with coefficients which are multiplied by eigenvalues raised to the power n. Eventually, only the eigenfunction with the largest eigenvalue will emerge, a property which is well-known. The algorithm is described by the figures and text in Papoulis' 1968 book.

Because the operation R uses a forward Fourier transform, a masking operation, an inverse Fourier transform, and another masking operation, the algorithm is similar to the iterative transform algorithm generally known as the Gerchberg-Saxton algorithm (Gerchberg and Saxton, 1972).

We emphasize that the functions $w(x,y)$ and $A(u,v)$ can be any desired shape, which gives us the opportunity to shape both the aperture and the search region.

3. Examples

A one-dimensional, unapodized aperture of width D has inverse Fourier transform, $a(x)$, a Sinc function with its first zero at $x_0 = \lambda/D$. We call x_0 the diffraction-limited spot size or, more simply, a DL element. The magnitude squared of $a(x)$ is $p(x)$, the one-dimensional point spread function (PSF). A square, two-dimensional aperture has $PSF = p(x)p(y)$. On the left in Figure 1 is the logarithm of the PSF for such an unapodized aperture. The diagonal line in the image shows where we will sample the PSF for comparison purposes. In all of our examples we assume that the available light is broadband with a bandwidth which

is 20% of the central wavelength. Thus, the deep nulls in a conventional Sinc function are blurred out when we combine the PSF's at various wavelengths.

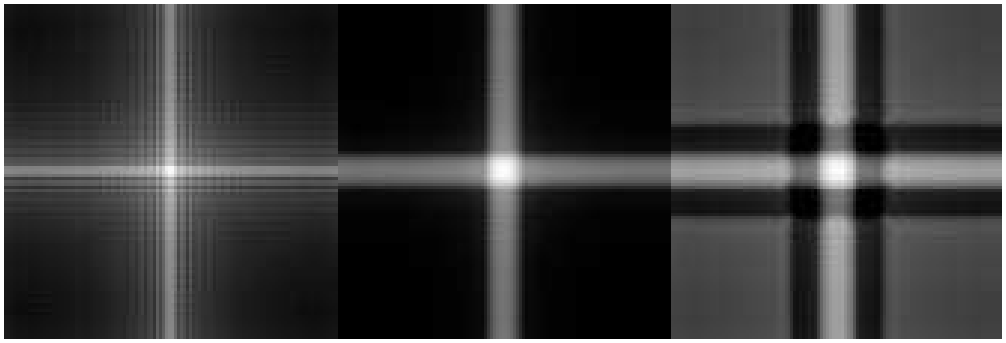

Fig. 1.— Logarithm of Point Spread Functions for three apodizers. Left: No apodizer; Center: Product Prolate Spheroidal (PPS) with a $4.4x_0$ by $4.4x_0$ central square; Right: Modified PPS

To form this first apodized aperture we space-limit a one-dimensional $f(x)$ to the interval, say, $-2.2x_0 < x < 2.2x_0$, then we band-limit the result to D. (For these examples, we used FFT software with a calculation size of N = 256 and we set the aperture size to D = 41.) These space and bandwidth limiting operations are defined by Equations (3) and (4). We repeat them until the iterations converge. What emerges is the prolate spheroidal function, $\phi(x)$. Its Fourier transform, $\Phi(u)$, is the apodizer. Following previous authors (i.e. Aime et al, 2002), we form the product aperture $P(u, v) = \Phi(u)\Phi(v)$, which we call a Product Prolate Spheroidal (PPS) aperture, and its inverse Fourier transform, p(x,y), is the telescope's PSF. In the center of Figure 1 is the logarithm of the PSF for this apodizer. Note that the PSF is concentrated along the x and y axes. The aperture has a transmission of 24.9%. Papoulis (1968) showed that this aperture best concentrates the PSF into a central square of size $4.4x_0$ by $4.4x_0$.

Figure 1 shows a third PSF. This was formed by defining a one-D spatial mask, $w(x)$, which is 1 in the range from 0 to $2.27x_0$, zero from $2.27x_0$ to $6x_0$ and 1 for all larger x;

and is symmetric about $x = 0$. The mask forces the PSF to be narrow, as above, but also allows it to rise outside a restricted search region from $2.27x_0$ to $6x_0$. We apply the same iterative algorithm, starting with the PPS apodizer and stopping the iterations when the transmission is (26.3%). The result is the PSF shown on the right of Figure 1.

Figure 2 shows a 45 deg cut through three PSF's. The horizontal axis plots diagonal distance in units of x_0 and the vertical axis plots the logarithm of $p(x, y)$, scaled such that $p(0, 0) = 1$. Figure 2 also shows the PSF for the unapodized aperture. Note that the PPS plot is about seven orders of magnitude below the no-apodizer plot, beyond about $3.5x_0$. The modified PPS plot matches the PPS plot from 0 to $3.5x_0$, drops about 2 db below it to about $8x_0$, then rises almost to the no-apodizer plot.

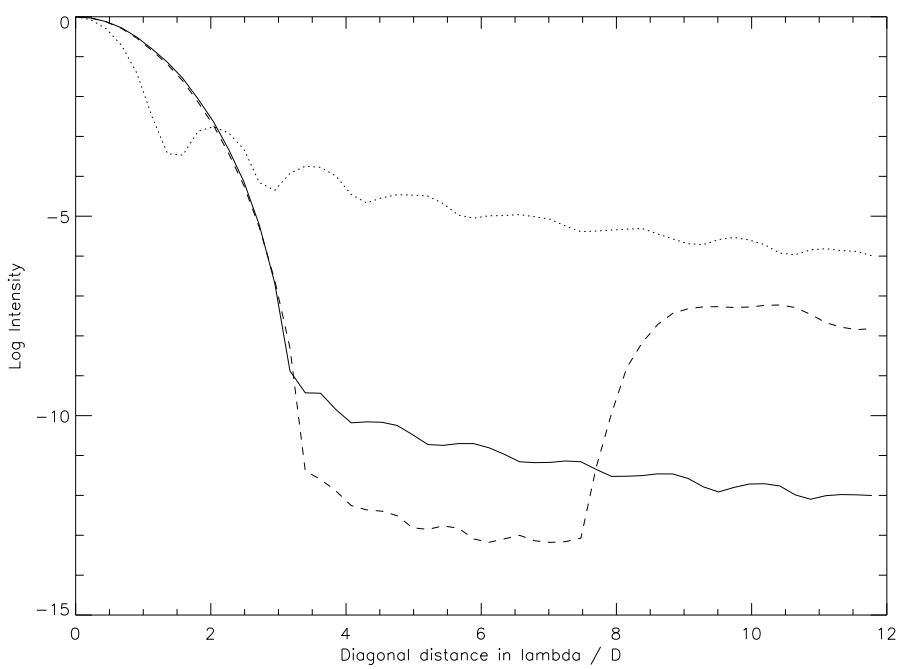

Fig. 2.— Slices of the PSF's vs. distance in Diffraction-Limited elements: No apodizer (dotted), Product Prolate Spheroidal Apodizer (solid), Modified PPS Apodizer (dashed)

Figure 3 shows horizontal cuts through the PPS apodizer and the modified PPS

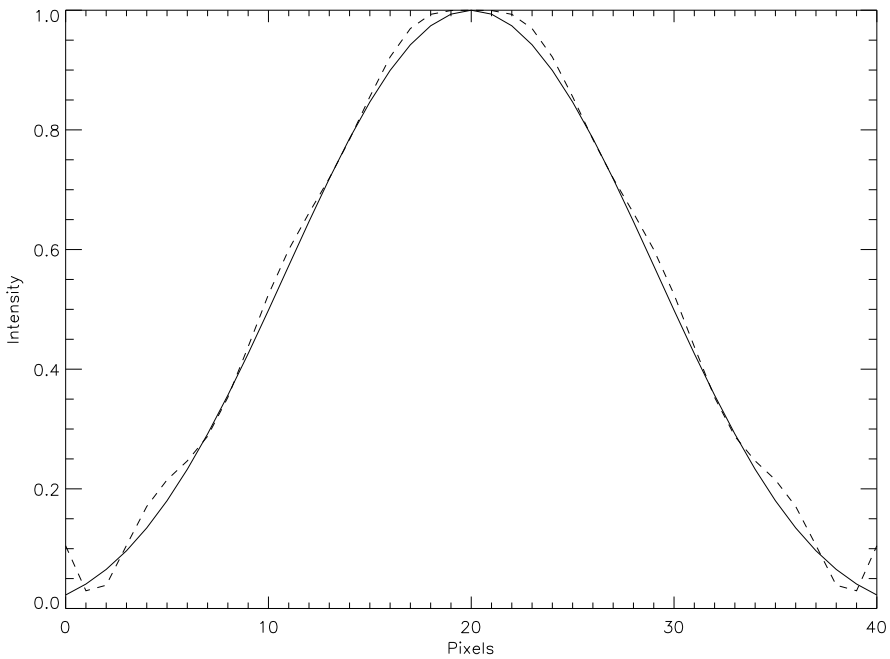

Fig. 3.— Prolate Spheroidal Apodizer (solid), Modified PS Apodizer (dashed)

apodizer.

For our next set of examples we used a circular aperture of diameter $D = 40$. First we calculated the PSF for an unapodized aperture. It is the well-known Airy disc. The logarithm of this PSF is shown on the left of Figure 4. (As in Figure 1 the PSF's are for wideband light so the rings are somewhat indistinct. The horizontal and vertical bands at the edge of the figures are aliasing, caused by our finite sampling.)

Next we formed a circular mask of radius 3.5z and exercised a two-dimensional version of the iterative algorithm. This results in the 2-D PSF in the center of Figure 4. This is the PSF which Papoulis (1968) reports but does not sketch. We call the apodizer a Circular Bessel (CB) apodizer. Then we allowed the mask to rise at a radius of $8.2x_0$, so that the mask looks like a bulls eye, and exercised the two-D algorithm. The PSF is on the right of Figure 4. Cuts through the PSF's are shown in Figure 5. Inside the search region the

bulls eye PSF is about two orders of magnitude below the PSF for the CB aperture. The apodizers are shown in Figure 6. Both have transmission of about 21% .

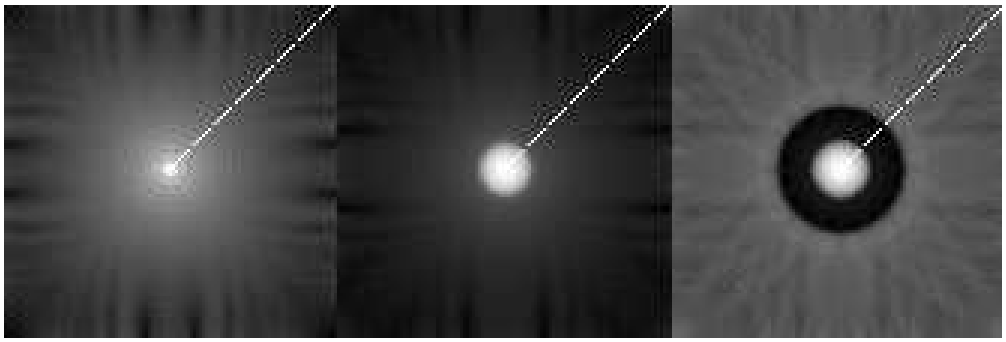

Fig. 4.— Log PSF's for no apodizer, CB apodizer, and Modified CB apodizer

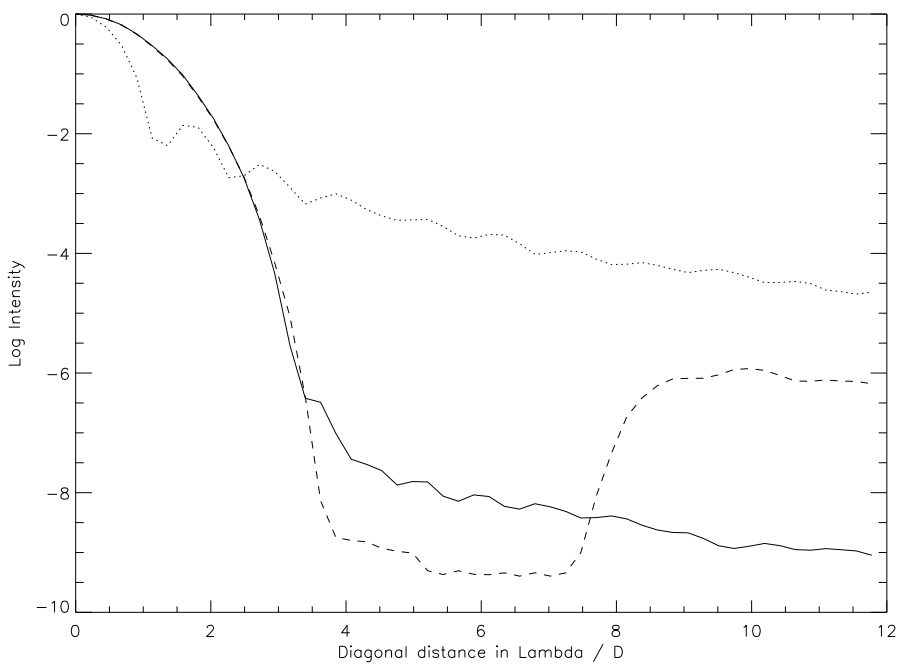

Fig. 5.— PSF slices for no apodizer (dotted), CB (solid), and Modified CB (dashed)

Finally, we formed an apodizer for a square aperture with a two-dimensional mask which is a cross of width $4x_0$, imbedded in a circular mask of radius $8x_0$, a hybrid apodizer. It has a restricted search area as shown on the left in Figure 7. We exercised the iterative

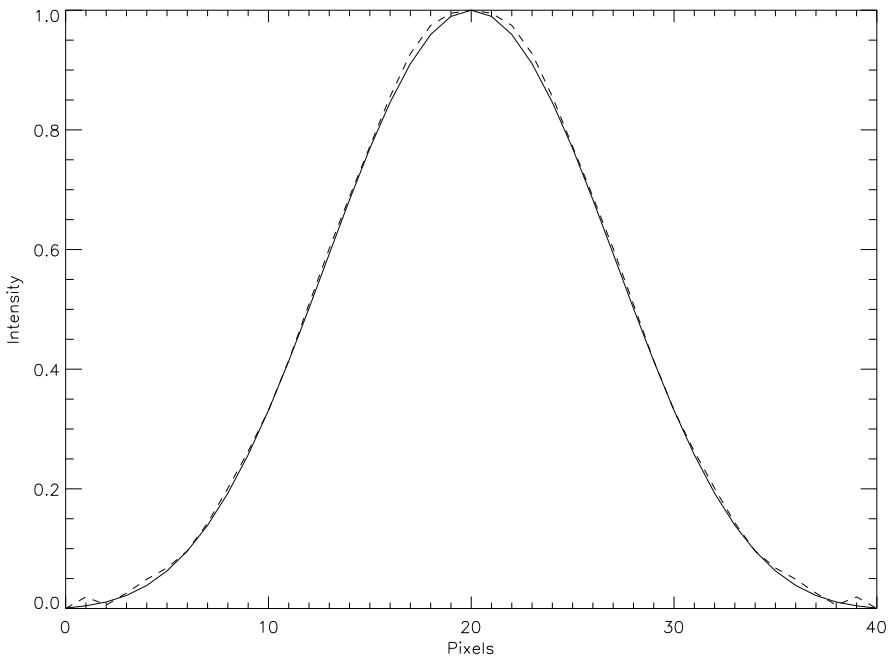

Fig. 6.— CB apodizer (solid), Modified CB apodizer (dashed)

algorithm, starting with the CB apodizer. Figure 7 shows the mask (the search area) and the log of the PSF. Figure 8 shows a slice through the PSF and, for comparison, a slice through the PSF for the CB apodizer. Despite what appear to be only subtle differences in the shapes of the two apodizers, the hybrid apodizer has a transmission of 39.3%, almost double that of the CB apodizer; it also has a narrower central peak and better sidelobe supression. The reduced search area of this hybrid apodizer provides significant advantages over our earlier examples. Figure 9 shows cuts through the apodizer at 0 and at 45 deg, which shows that the hybrid apodizer is not circularly symmetric.

4. Discussion

We have described an approach to designing an apodization mask that is optimized for minimizing diffraction in a selected local area of the focal plane. This would allow

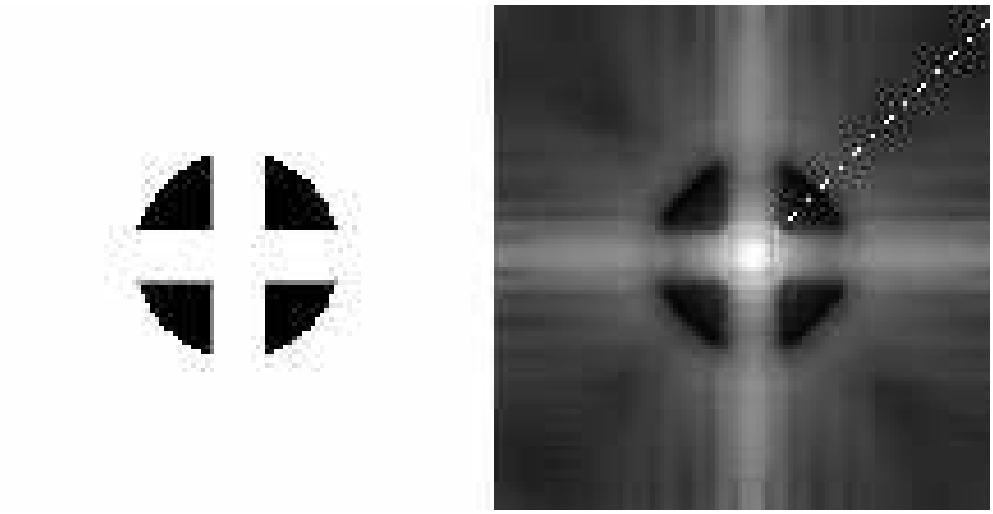

Fig. 7.— Spatial mask and the log PSF for a hybrid apodizer, matched to the mask

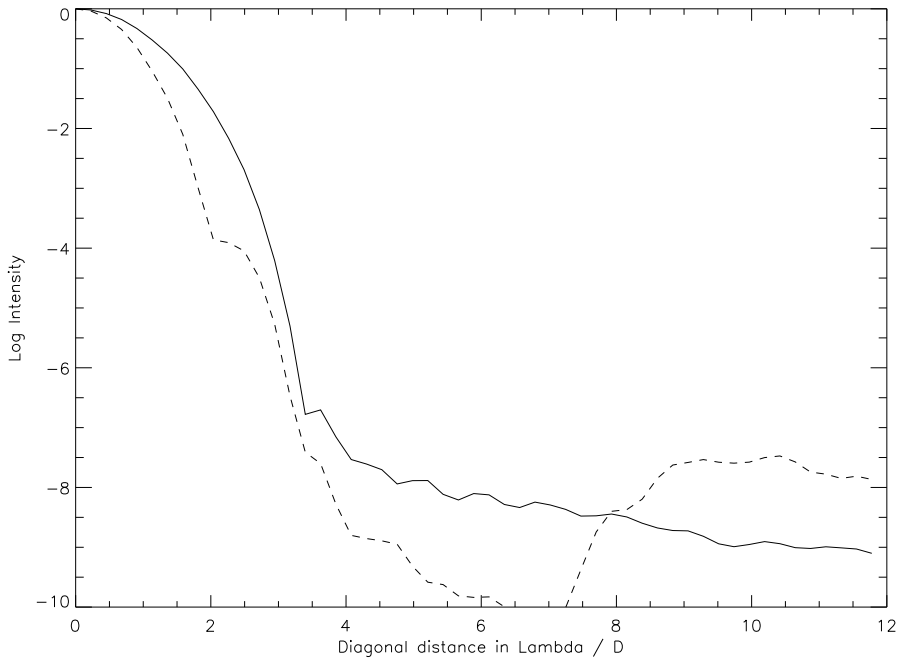

Fig. 8.— PSF cuts: CB apodizer, $Trans = 21.7\%$ (solid) ; Hybrid apodizer, $Trans = 39.3\%$ (dashed)

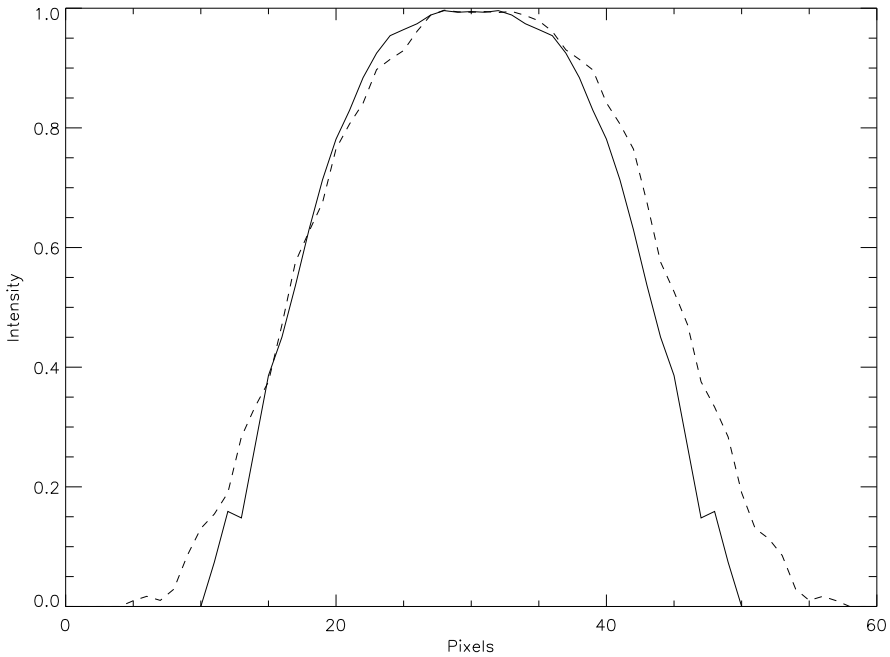

Fig. 9.— Hybrid apodizer at 0 deg (solid) and at 45 deg (dashed)

use of selectable apodization masks in a TPF telescope that could, for example, reduce diffraction over a wide area in the focal plane for a survey, and then produce deeper nulls in local areas for spectroscopy of an already detected planet. Or one could select an apodizer for the minimum width of the central peak, trading off the size of the searchable region for minimum detectable separation of star and planet. We also investigated use of apodizers that vary only in one direction (constant in the other). These apodizers result in maximizing throughput (close to 50%) while allowing detection of luminosity ratios of 10^8. This is insufficient for TPF-like missions (luminosity ratios will be of order 10^{10} for an earth-like planet orbiting a star at 10 pc) but hybrid apodizers, as described in the paper, allow a continuous trade-off between maximizing throughput and minimizing diffraction.

The speckle due to optical surface errors and the diffraction will produce a PSF that is highly centro-symmetric when (as required for a TPF telescope) the phase errors

are extremely small. For very small phases, the exponential phase can be accurately approximated by only the linear term of the power series expansion of the exponential. So, for example, a telescope with 1/1000 wave rms surface errors will have a centro-symmetric psf to a precision of about 0.1% and 1/10000 wave results in centro-symmetry of 0.01%. One can then use this asymmetry to calibrate the residual speckle and diffraction in the half-plane of the PSF that contains a planet using the opposite half-plane. Subtraction of the calibration region then increases the dynamic range to an accuracy limited only by photon statistics.

Accurate intensity transmission of the apodizers is critical for their success - this is evident from the apparently small differences in apodizer shape, as illustrated in Figure 3, producing substantial effects on the PSF. We have estimated the precision required in the transmission of the apodizer to be 0.3% or better for it not to affect the dynamic range. This is the same requirement as one for the uniformity of the reflective coatings of the telescope mirrors. Numerical simulations that substantiate this result are included in Nisenson et al. (2003)

The usual problems with iterative algorithms are choosing an initial function and choosing a stopping point in the iterations. For the examples which yielded the PS and CB solutions, we started with a Gaussian shape and we stopped the iterations when there was no significant change in the solution, typically a few hundred iterations. For the other examples we started with a PS or CB aperture. Continued iterations result in deeper and deeper suppression of diffraction in the chosen region but also resulted in decreasing throughput for the apodizer. We stop the iterations when the diffraction is reduced to a selected level while leaving the throughput at a maximum.

We have shown an approach to calculating an optimum apodizer that maximizes the detectable luminosity ratio for exo-planet detection in the focal plane of the TPF telescope.

The next step in this analysis would be to include realistic specifications on wavefront errors from the telescope optics and also to factor in practical limits on the accuracy in the manufacture of apodizing masks. How well continuous tone apodizers can be manufactured is an open question. Many of the techniques developed for photolithography allow very precise shaped transmission to be generated in special glass. Such a mask was used in a laboratory demonstration of imaging two close point sources with a luminosity ratio of nearly 10^9 (Melnick et al, 2001).

REFERENCES

Aime C., Soummer R. and Ferrari A. 2001, A & A **379**, p697.

Aime C., Soummer R. and Ferrari A. 2002, A & A **389** p334.

Gerchberg R.W. and Saxton W.O.,1972, "Practical algorithm for determination of phase from image and diffraction plane pictures," Optik **35**, p237.

Kaiser J.F. 1966, "Digital Filters, "System Analysis by Digital Computer", Chapter 7, Kuo, F.F. and Kaiser, J.F., Eds. John Wiley and Sons, New York, NY.

Kasdin N.J., Spergel D.N., and Littman M.G. 2002, submitted to Applied Optics.

Melnick, G. J., Fischer, D., Geary, J. C., Gezari, D. Y., Hardesty, C., Harwit, M., Holman, M., Korzennik, S. G., Lyon, R. G., Marley, M. S., McElroy, M. B., Neufeld, D. A., Nisenson, P., Noyes, R. W., Papaliolios, C., Ridgway, S. T., Sasselov, D. D. 2001, American Astronomical Society Meeting 199, #09.10.

Nisenson, P. and Papaliolios, C. 2001, ApJ, **548**, L201.

Nisenson, P., Melnick, G.J., Geary, J., Holman, M. Korzennik, S.G., Noyes, R.W., Papaliolios, C., Sasselov, D.D., Gonsalves, R., Hardesty, C, Gezari, D., Lyon, R.G., Fischer, D., Harwit, M., Marley, M.S., Neufeld, D.A., Ridgway, S.T. 2003, to appear in ASP Conf. Ser., Scientific Frontiers on Research of Extrasolar Planets, eds. D. Deming & S. Seager, (San Francisco: ASP).

Oppenheim A.V. and Schafer R.W. 1989, Discrete-Time Signal Processing, Prentice Hall, Englewood Cliffs, NJ.

Papoulis, A. 1968, Systems and transforms with applications in optics (New York: McGraw-Hill).

Slepian, D. and Pollak, O.P. 1961, The Bell System Technical Journal.

von Neumann, J. 1950, Annals of Math. Studies, No. 22, Princeton University Press, a reprint of lecture notes from 1933.

This manuscript was prepared with the AAS LaTeX macros v5.0.